

Supporting Information

Structures of Potassium Calix[4]arene Crown Ether Inclusion Complexes and Application in Polymerization of *rac*-Lactide

*Yingguo Li, Hongwei Zhao, Xiaoyang Mao, Xiaobo Pan, Jincui Wu**

Key Laboratory of Nonferrous Metal Chemistry and Resources Utilization of Gansu Province, State Key Laboratory of Applied
Organic Chemistry, College of Chemistry and Chemical Engineering, Cuiying Honors College, Lanzhou University, Lanzhou 730000,
People's Republic of China

Table of Contents

Figure S1. Molecular structure of complex **1** (**1D** zigzag polymeric chain).

Figure S2. ^1H NMR spectra (Toluene- d_8) recorded at different temperatures of complex **2**.

Figure S3. ^1H NMR spectra (CDCl_3) recorded at different temperatures of complex **3**.

Figure S4. Molecular structure of complex **3** (two different molecular structures in one asymmetric unit).

Figure S5. Comparison of complex **1** + **BnOH** (excess) and complex **2** + **BnOH** (excess) on ^1H NMR spectrum (C_6D_6 , 25°C).

Figure S6. Comparison of complex **2**, complex **2** + **BnOH** (2 equiv.) and complex **2** + **BnOH** (excess) on ^1H NMR spectrum (C_6D_6 , 25°C).

Figure S7. Polymerization of *rac*-LA catalyzed by complex **2** in toluene at room temperature. The relationships between PDI(■), Mn (□) of the polymer and the initial mole ratios $[\text{LA}]_0/[\text{BnOH}]_0$ (Table 1, entries 1, 7, 8, 9) is shown.

Figure S8. Polymerization of *rac*-LA catalyzed by complex **3** in toluene at room temperature. The relationships between PDI(■), Mn (□) of the polymer and the initial mole ratios $[\text{LA}]_0/[\text{BnOH}]_0$ (Table 1, entries 17, 20-23) is shown.

Figure S9. Methine region of the (a) ^1H NMR spectrum (b) ^{13}C NMR spectrum (CDCl_3 , 400 MHz) of the poly(*rac*-lactide) produced from *rac*-LA using complex **3** (Table 1, entry 25). Methine region of the (c) homonuclear decoupled ^1H NMR spectrum (CDCl_3 , 400 MHz) (d) ^{13}C NMR spectrum (CDCl_3 , 400 MHz) of the poly(*L*-lactide) produced from *L*-LA using complex **3** (Table 1, entry 26). The P_m values determined by homonuclear decoupled ^1H NMR and ^{13}C NMR of the methine region.

Figure S10. ^1H NMR analysis of poly (*rac*-LA) obtained from polymerization of *rac*-LA initiated by complex **3** (Table 1, entry 17).

Figure S11. Enlarged ESI-MS spectrum of poly(*rac*-LA) prepared by ROP of *rac*-LA (Table 1, entry 17).

Figure S12. ^1H NMR spectrum (CDCl_3 , 25°C) of complex **1**.

Figure S13. ^{13}C NMR spectrum (CDCl_3 , 25°C) of complex **1**.

Figure S14. ^1H NMR spectrum (C_6D_6 , 25°C) of complex **2**.

Figure S15. ^{13}C NMR spectrum (C_6D_6 , 25°C) of complex **2**.

Figure S16. ^1H NMR spectrum (CDCl_3 , 25°C) of complex **3**.

Figure S17. ^{13}C NMR spectrum (CDCl_3 , 25°C) of complex **3**.

Figure S18. ^1H NMR spectrum (C_6D_6 , 25°C) of complex **4**.

Figure S19. ^{13}C NMR spectrum (C_6D_6 , 25°C) of complex **4**.

Table S1. Details of the X-ray structure Determinations of Complexes **1-4**.

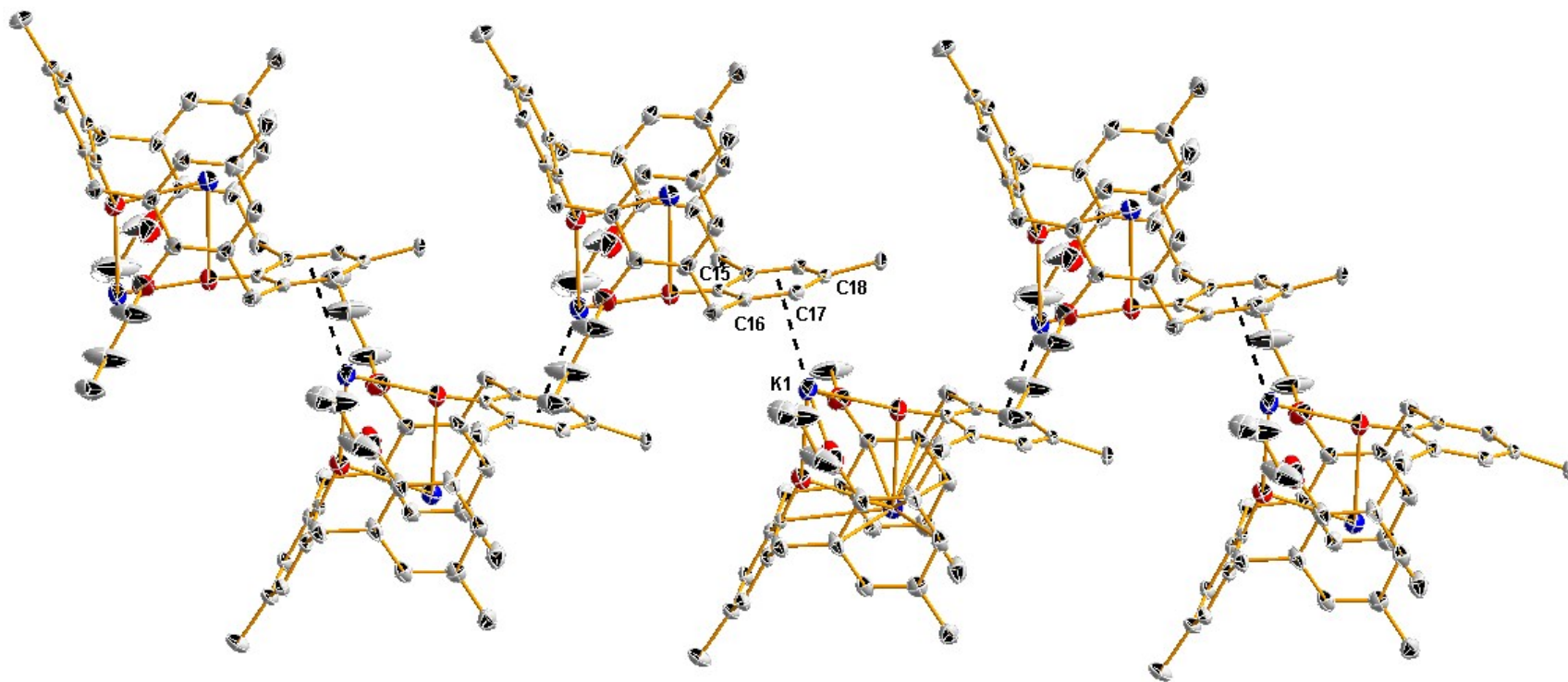


Figure S1. Molecular structure of complex **1** (**1D** zigzag polymeric chain).

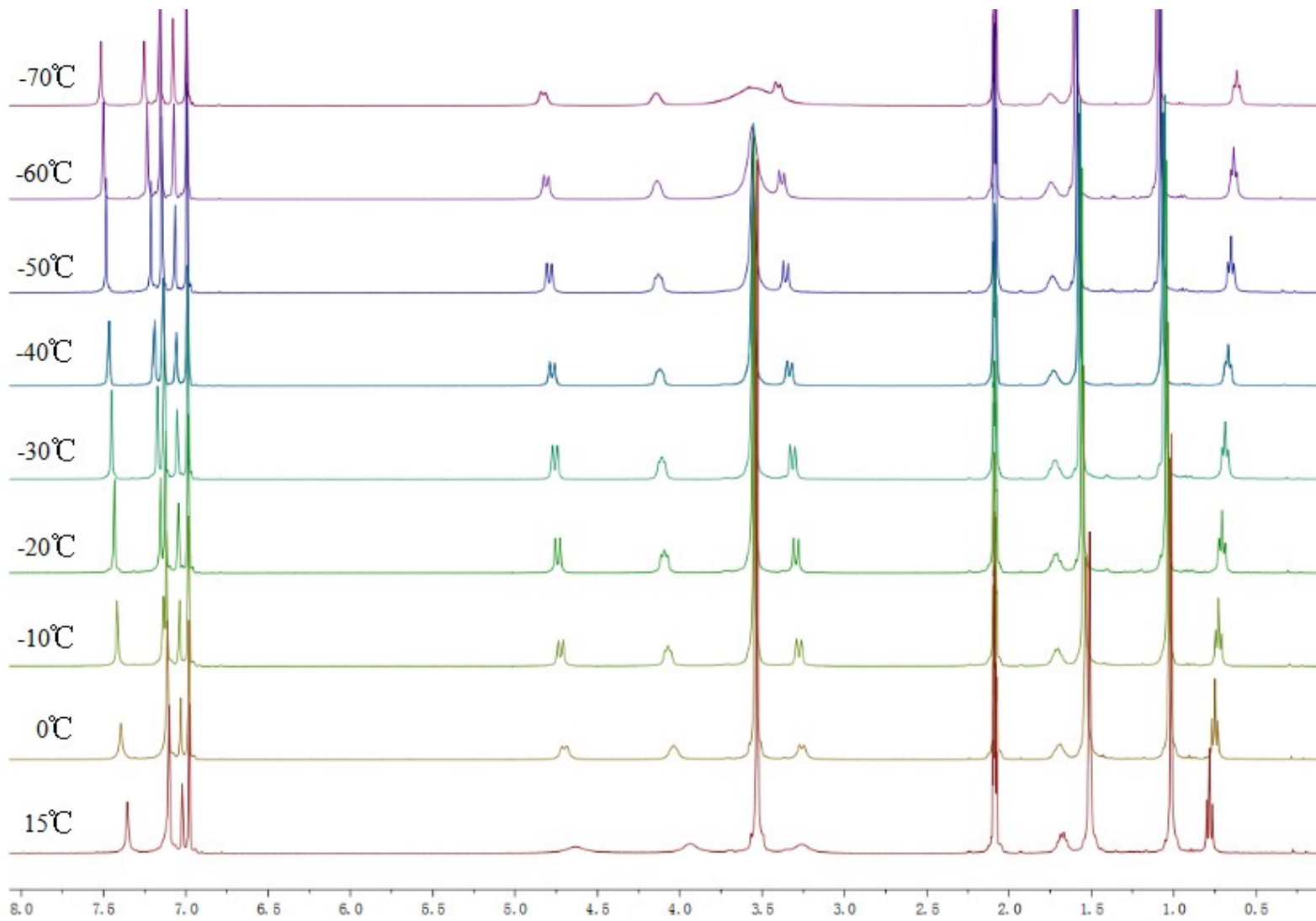


Figure S2. ^1H NMR spectra (Toluene-d_8) recorded at different temperatures of complex 2.

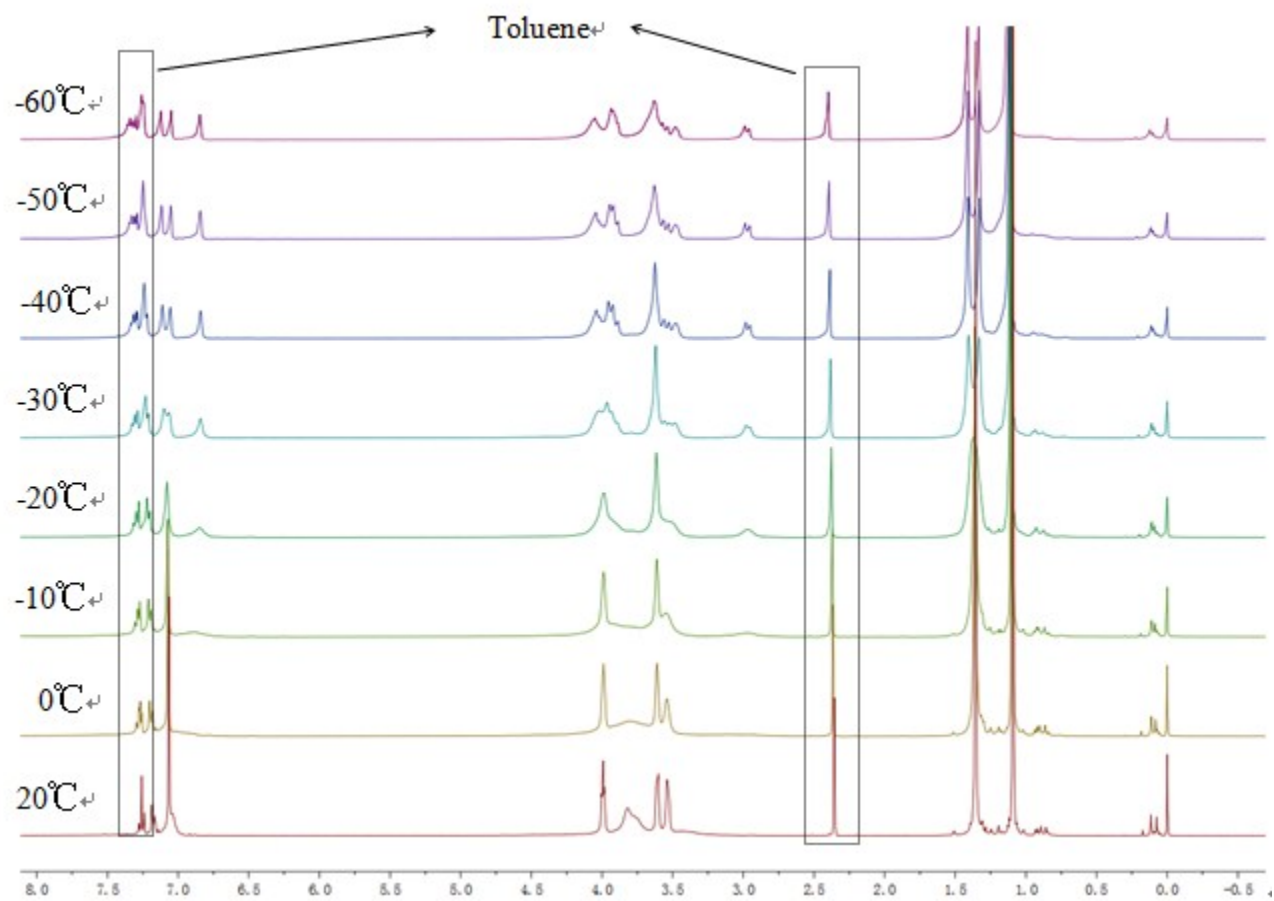


Figure S3. ^1H NMR spectra (CDCl_3) recorded at different temperatures of complex **3**.

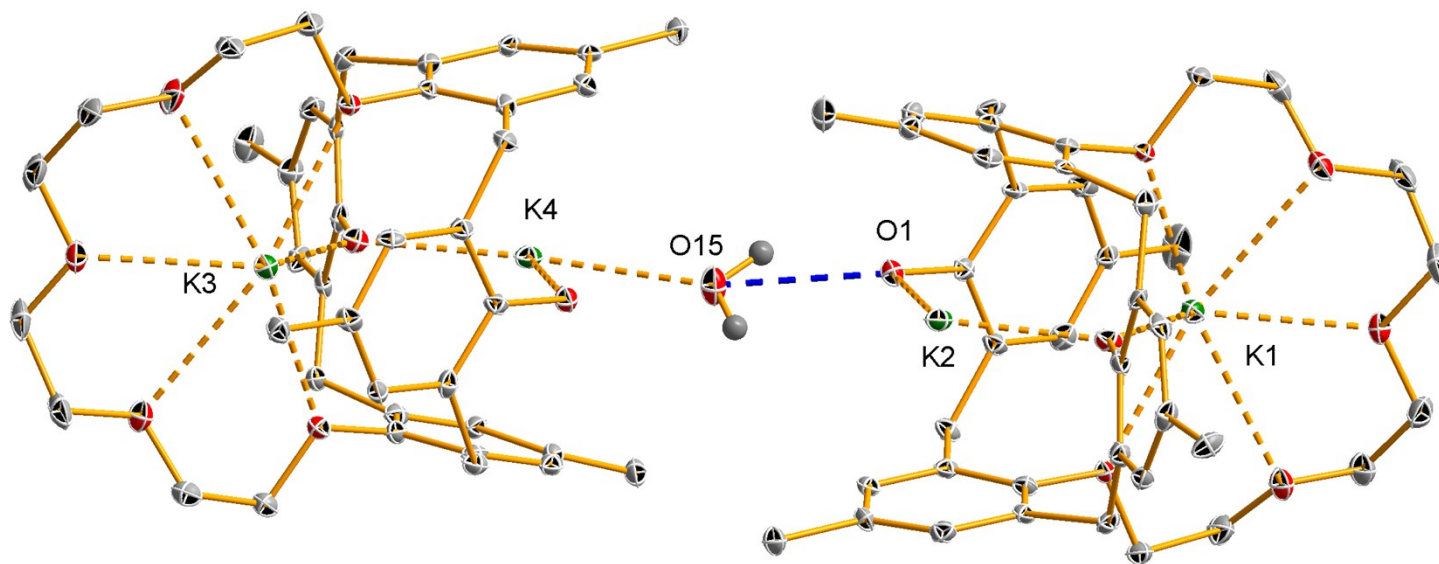


Figure S4. Molecular structure of complex **3** (two different molecular structures in one asymmetric unit).

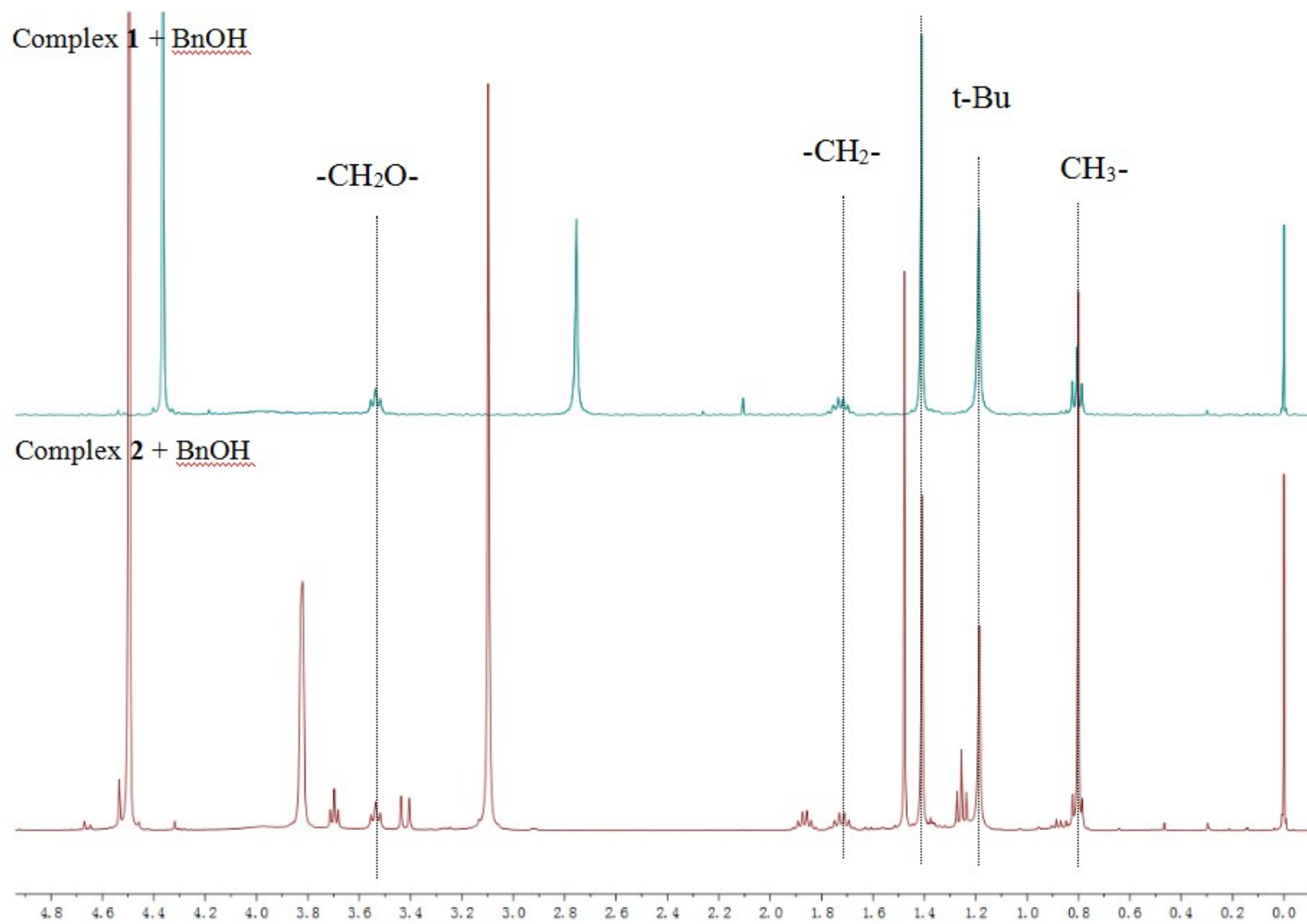


Figure S5. Comparison of complex **1** + **BnOH** (excess) and complex **2** + **BnOH** (excess) on ¹H NMR spectrum (C₆D₆, 25°C).

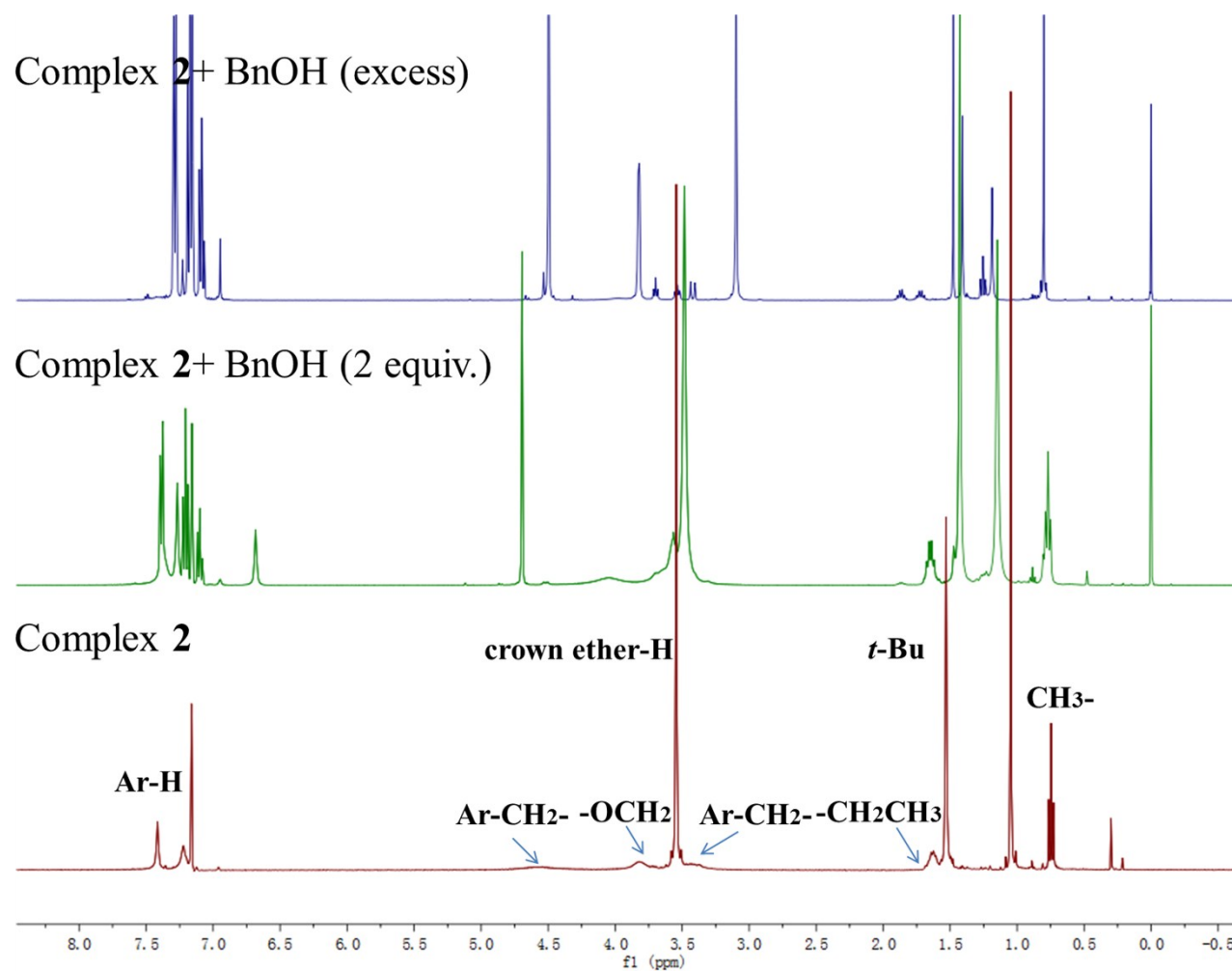


Figure S6. Comparison of complex **2**, complex **2** + **BnOH** (2 equiv.) and complex **2** + **BnOH** (excess) on ¹H NMR spectrum (C₆D₆, 25°C).

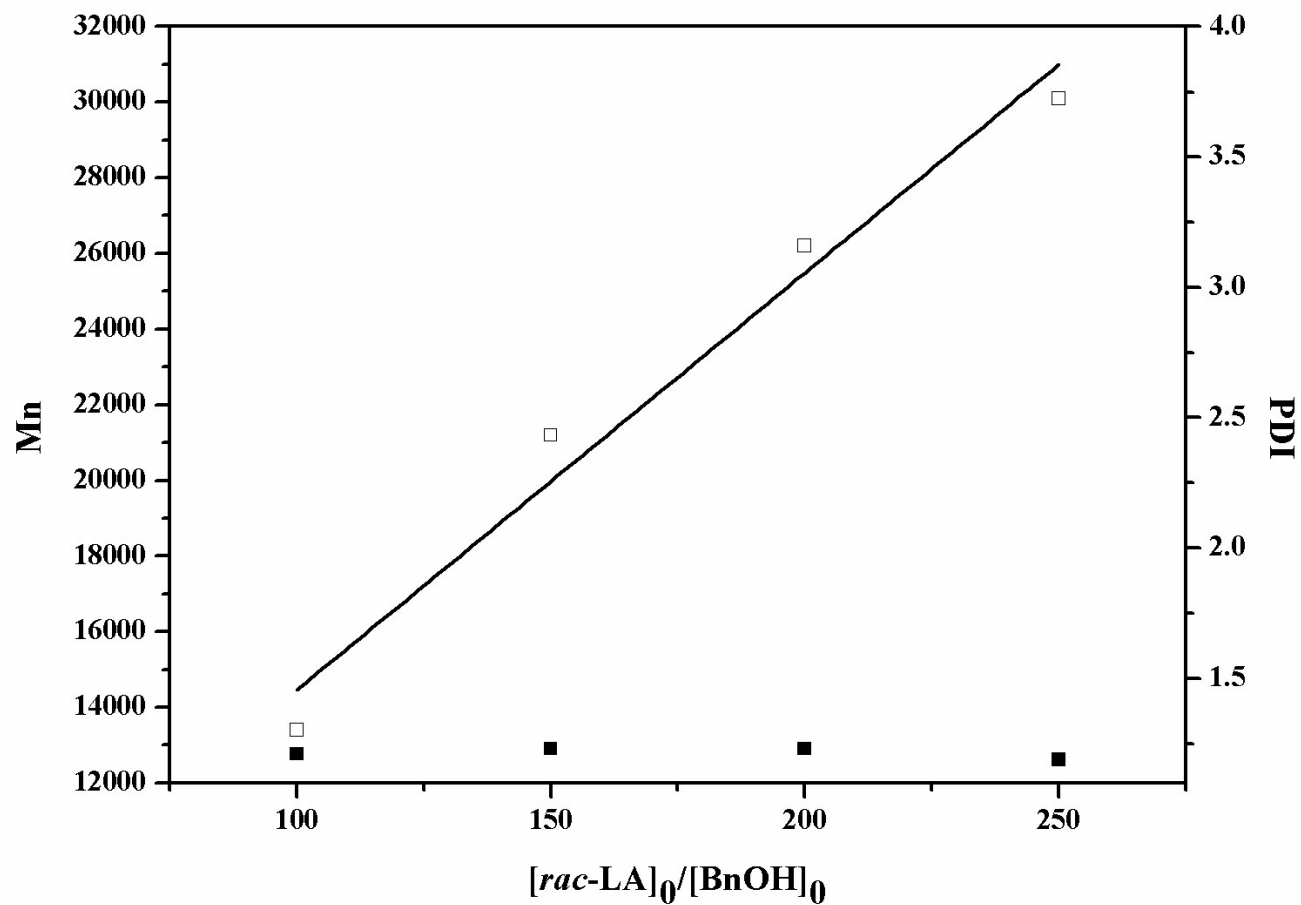


Figure S7. Polymerization of *rac*-LA catalyzed by complex **2** in toluene at room temperature. The relationships between PDI(■), Mn (□) of the polymer and the initial mole ratios $[LA]_0/[BnOH]_0$ (Table 1, entries 1, 7, 8, 9) is shown.

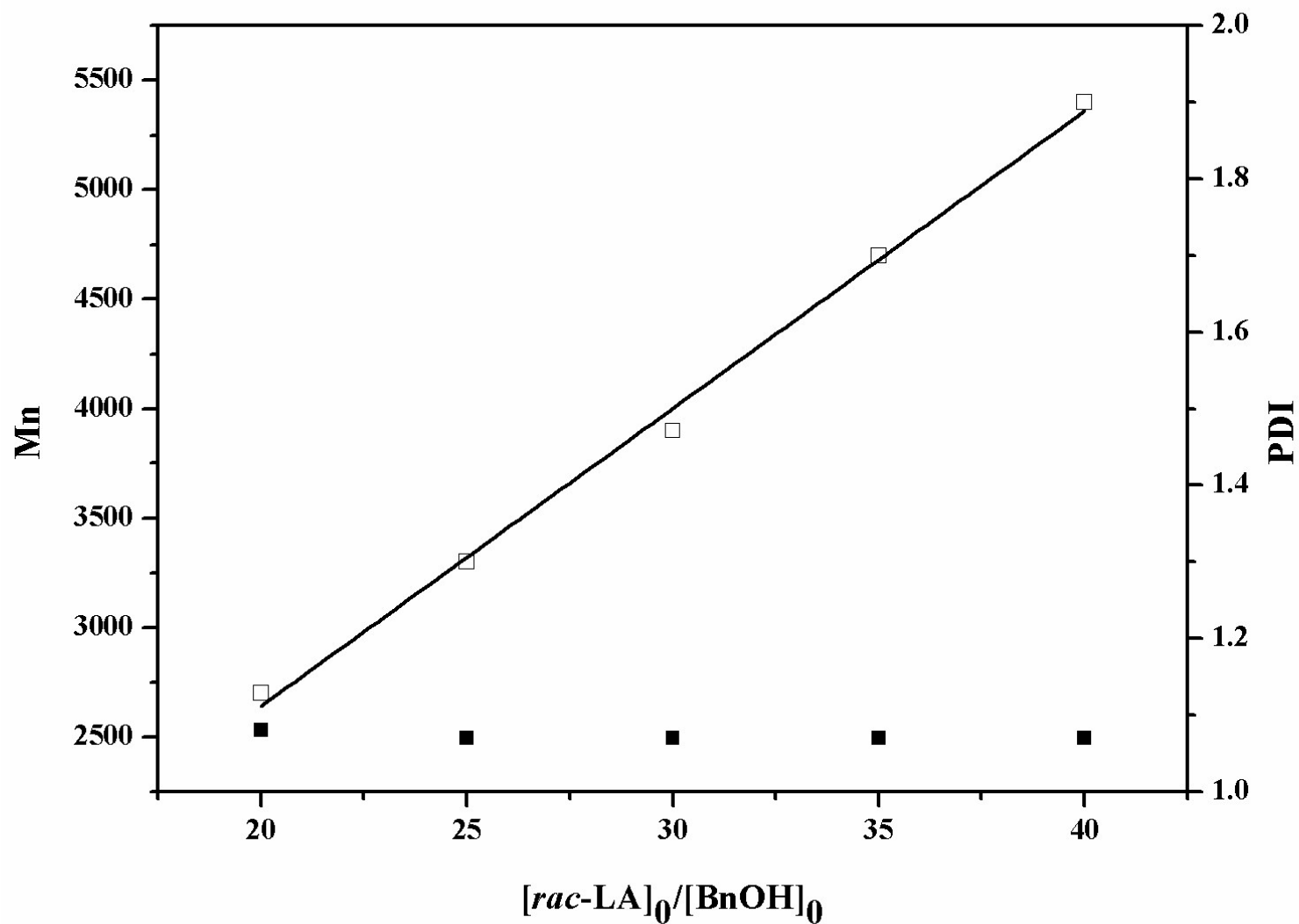


Figure S8. Polymerization of *rac*-LA catalyzed by complex **3** in toluene at room temperature. The relationships between PDI (■) , M_n (□) of the polymer and the initial mole ratios $[LA]_0/[BnOH]_0$ (Table 1, entries 17, 20-23) is shown.

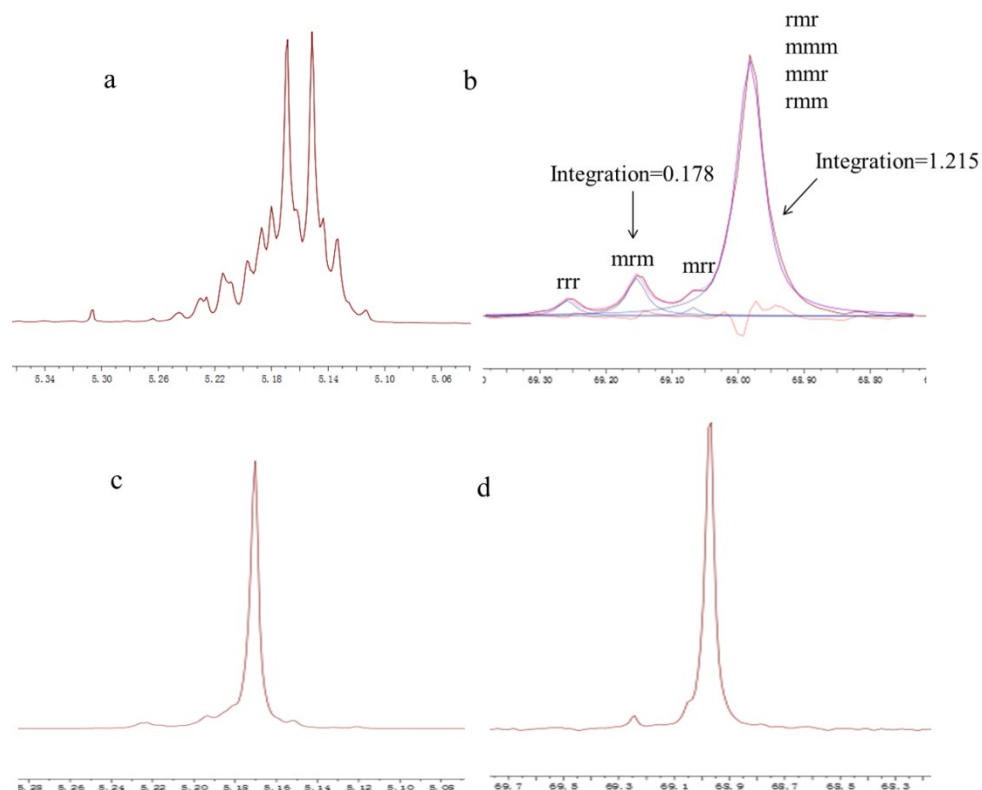


Figure S9. Methine region of the (a) ^1H NMR spectrum (b) ^{13}C NMR spectrum (CDCl_3 , 400 MHz) of the poly(*rac*-lactide) produced from *rac*-LA using complex **3** (Table 1, entry 25). Methine region of the (c) homonuclear decoupled ^1H NMR spectrum (CDCl_3 , 400 MHz) (d) ^{13}C NMR spectrum (CDCl_3 , 400 MHz) of the poly(*L*-lactide) produced from *L*-LA using complex **3** (Table 1, entry 26). The P_m values determined by homonuclear decoupled ^1H NMR and ^{13}C NMR of the methine region.¹

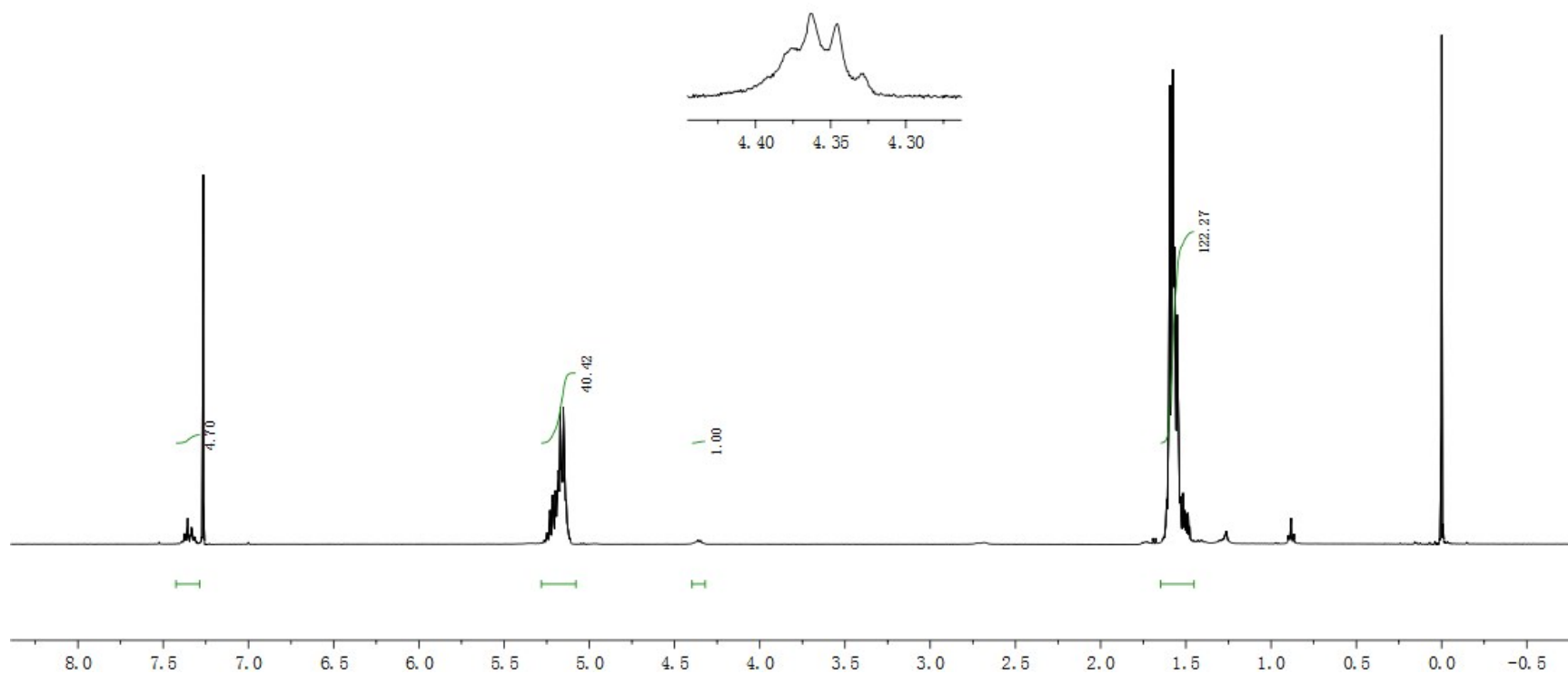


Figure S10. ¹H NMR analysis of the small molecular weight poly(*rac*-LA) obtained from polymerization of *rac*-LA initiated by complex **3** (Table 1, entry 17, $[LA]_0/[cat.]_0/[BnOH]_0 = 200:1:10$)

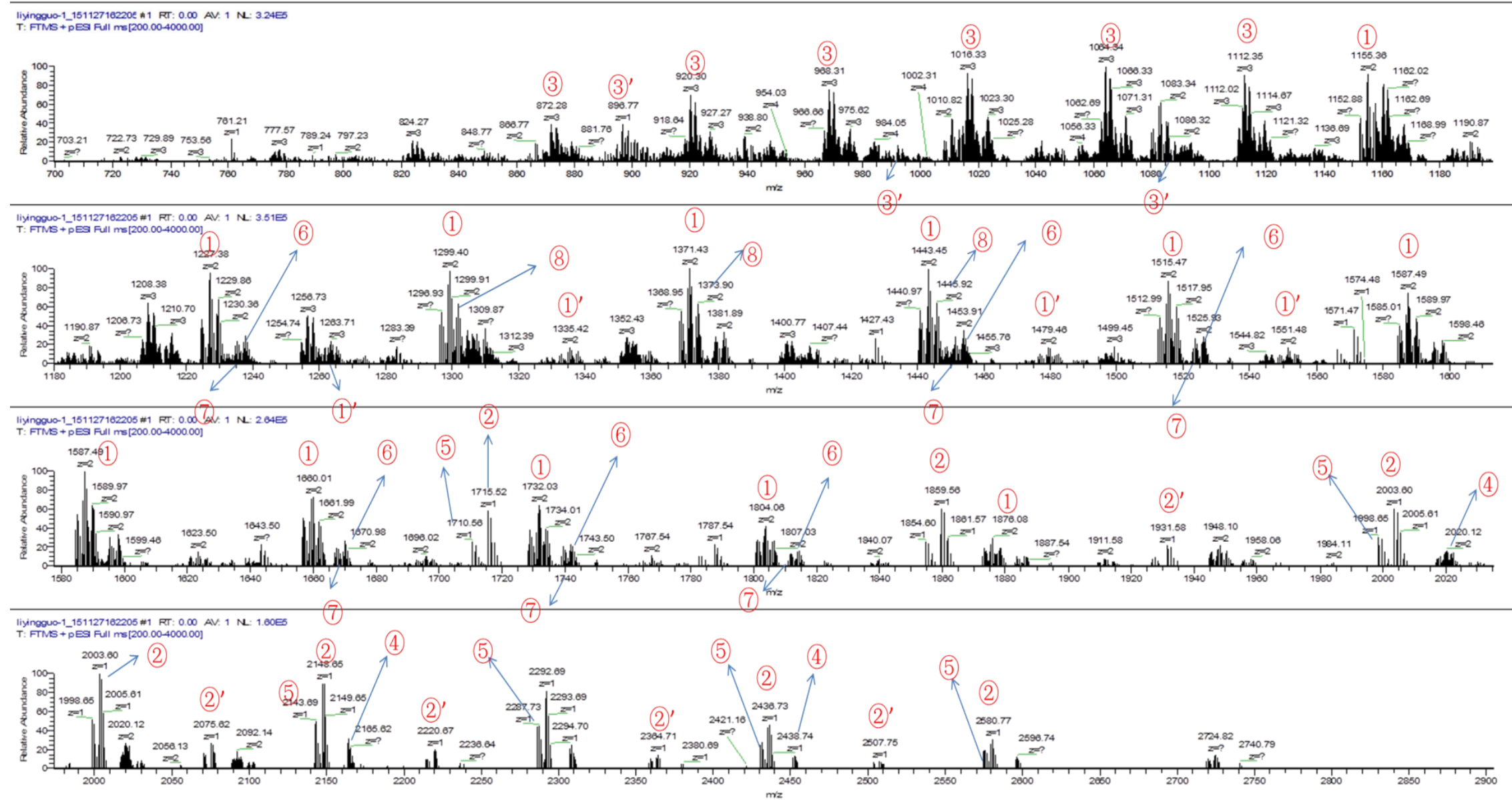


Figure S11. Enlarged ESI-MS spectrum of poly(*rac*-LA) prepared by ROP of *rac*-LA (Table 1, entry 17)

In EMS-MS spectrum:

- | | |
|--|--|
| ①: $144.04n + \text{BnOH} + \text{Na}^+ + \text{H}_3\text{O}^+$ | ①': $144.04n + \text{BnOH} + \text{Na}^+ + \text{H}_3\text{O}^+ + 72.02$ |
| ②: $144.04n + \text{BnOH} + \text{Na}^+$ | ②': $144.04n + \text{BnOH} + \text{Na}^+ + 72$ |
| ③: $144.04n + \text{BnOH} + \text{Na}^+ + 2\text{H}_3\text{O}^+$ | ③': $144.04n + \text{BnOH} + \text{Na}^+ + 2\text{H}_3\text{O}^+ + 72$ |
| ④: $144.04n + \text{BnOH} + \text{K}^+$ | ⑤: $144.04n + \text{BnOH} + \text{NH}_4^+$ |
| ⑥: $144.04n + \text{BnOH} + \text{Na}^+ + \text{K}^+$ | ⑦: $144.04n + \text{BnOH} + \text{K}^+$ |
| ⑧: $144.04n + \text{BnOH} + 2\text{Na}^+$ | |

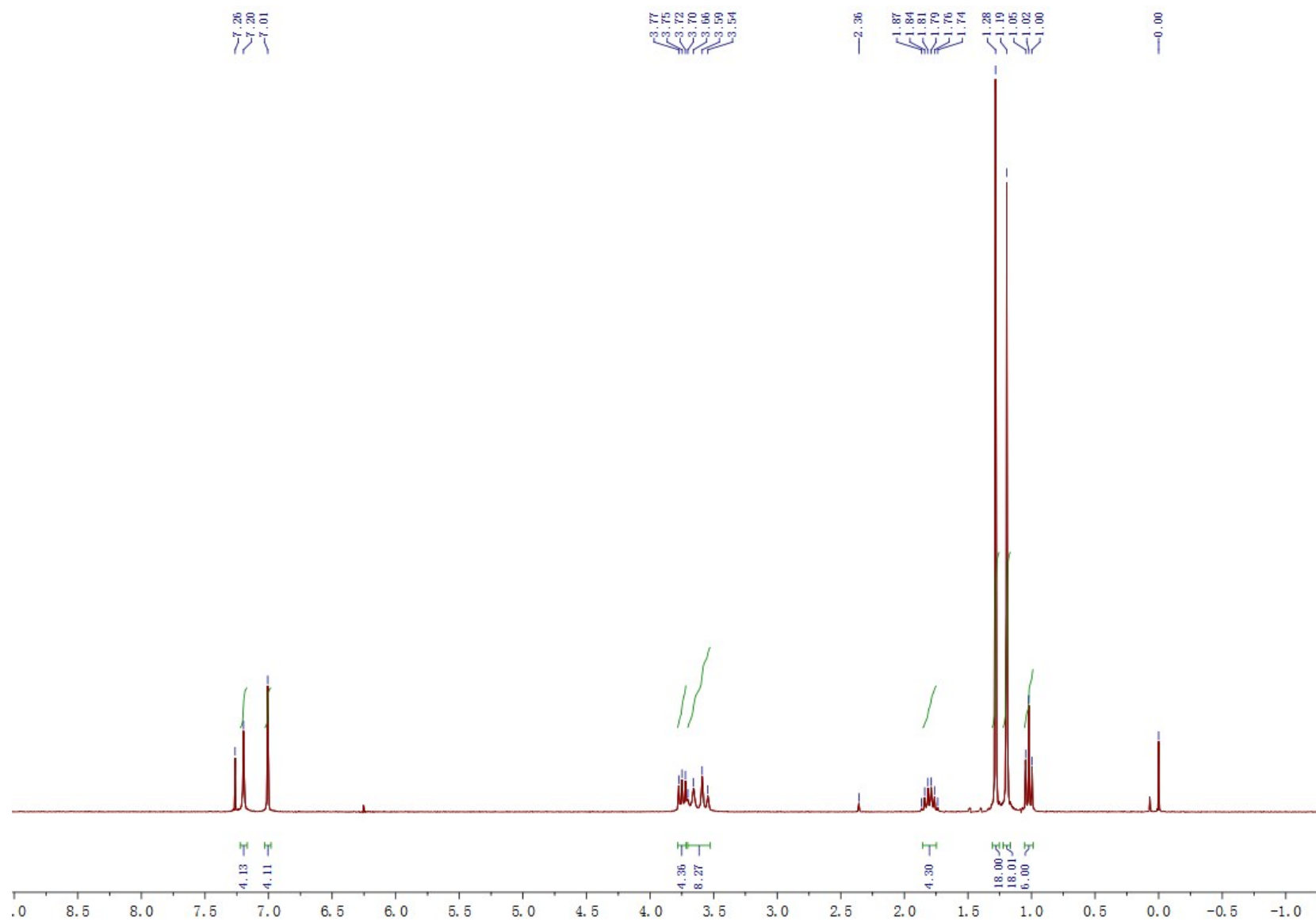


Figure S12. ¹H NMR spectrum (CDCl₃, 25°C) of complex 1.

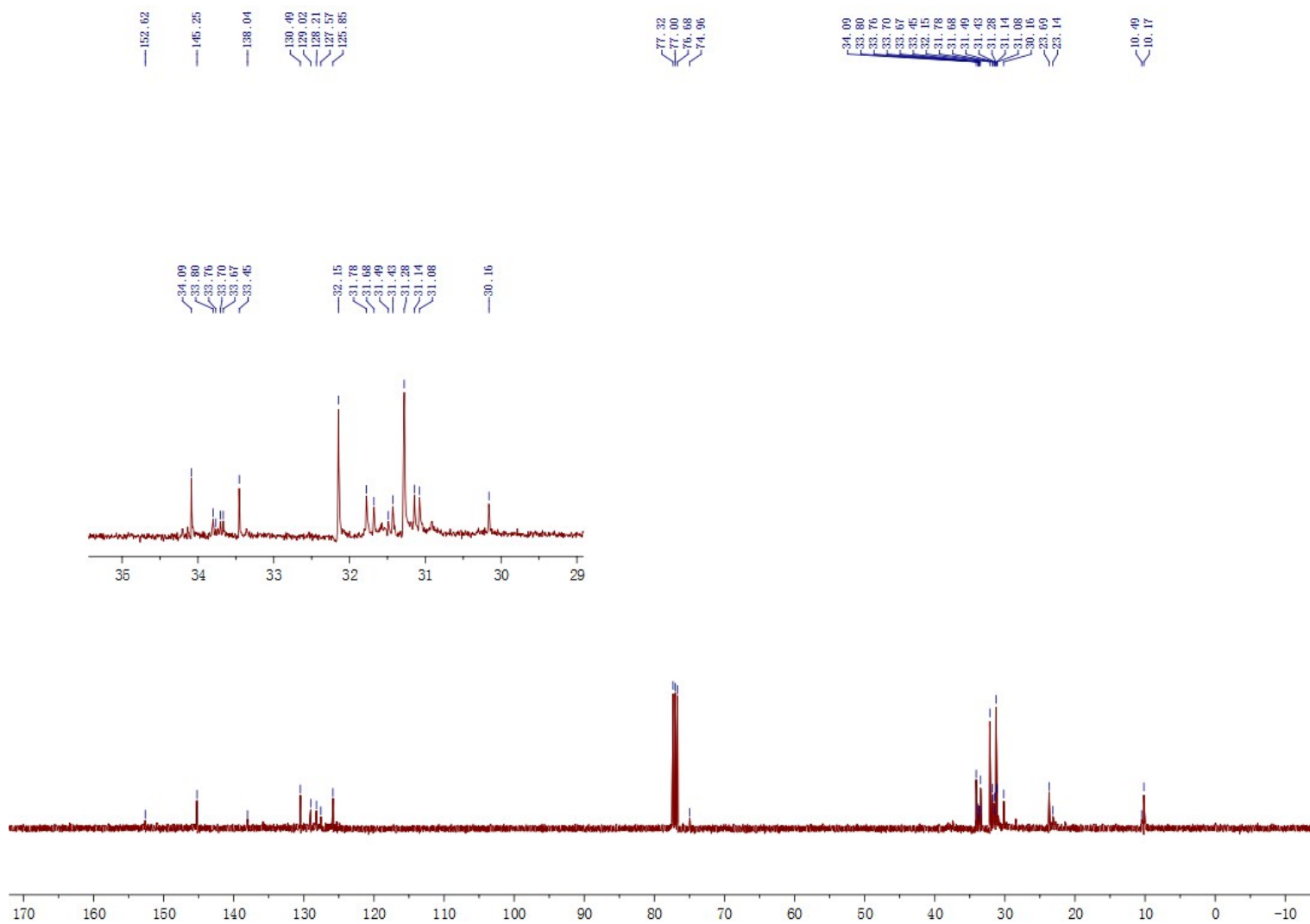


Figure S13. ^{13}C NMR spectrum (CDCl_3 , 25°C) of complex **1**.

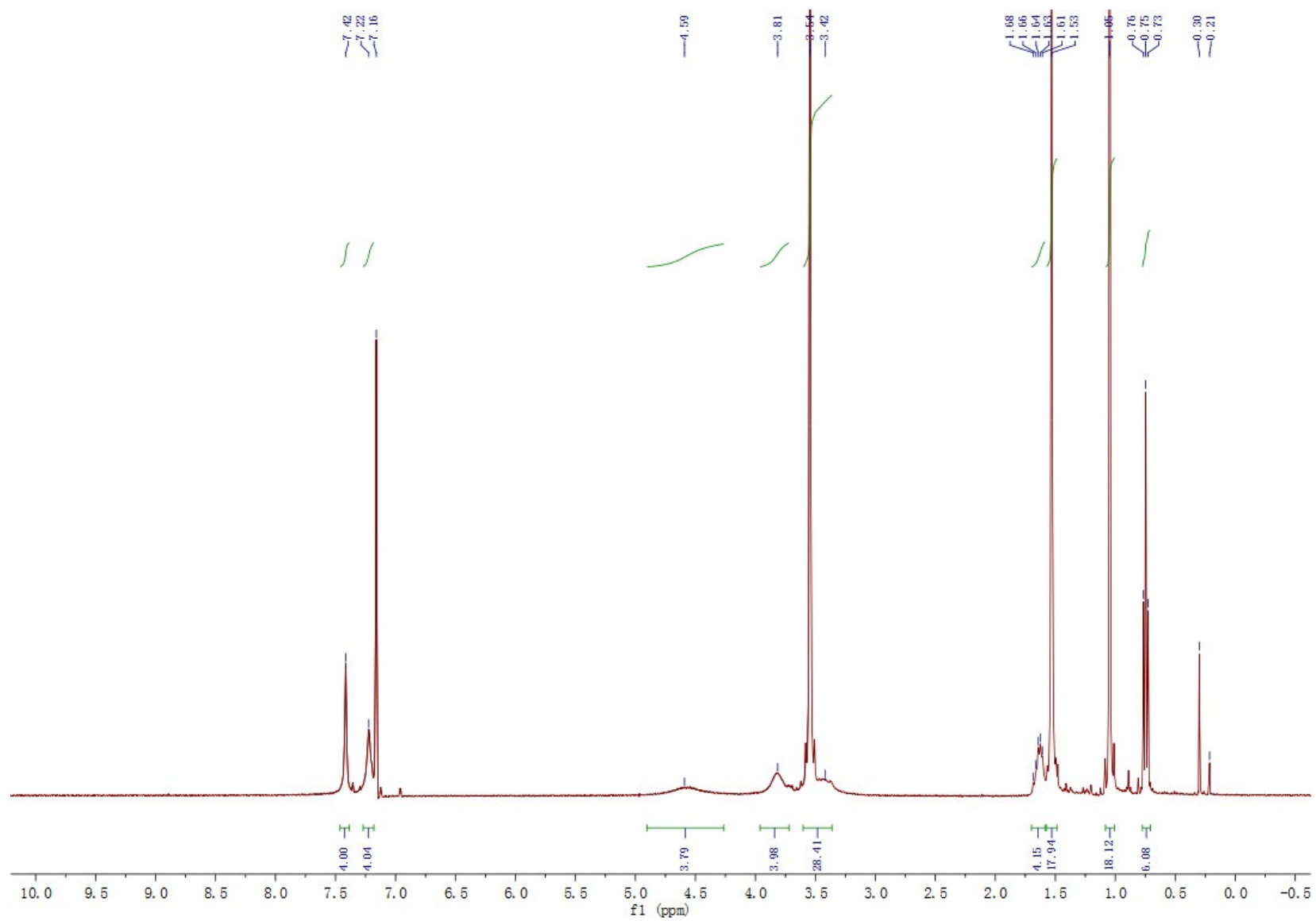


Figure S14. ¹H NMR spectrum (C₆D₆, 25°C) of complex 2.

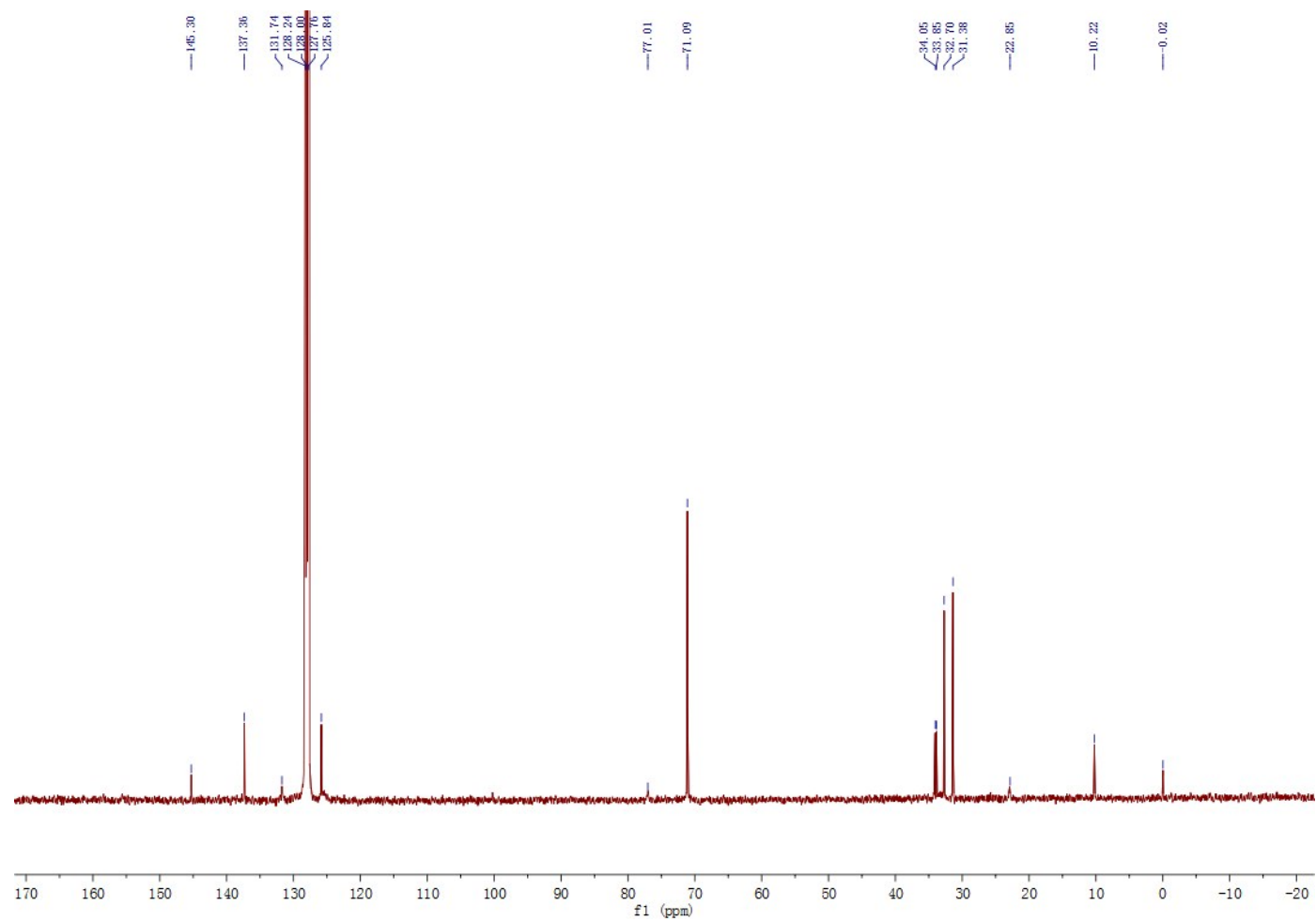


Figure S15. ^{13}C NMR spectrum (C_6D_6 , 25°C) of complex 2.

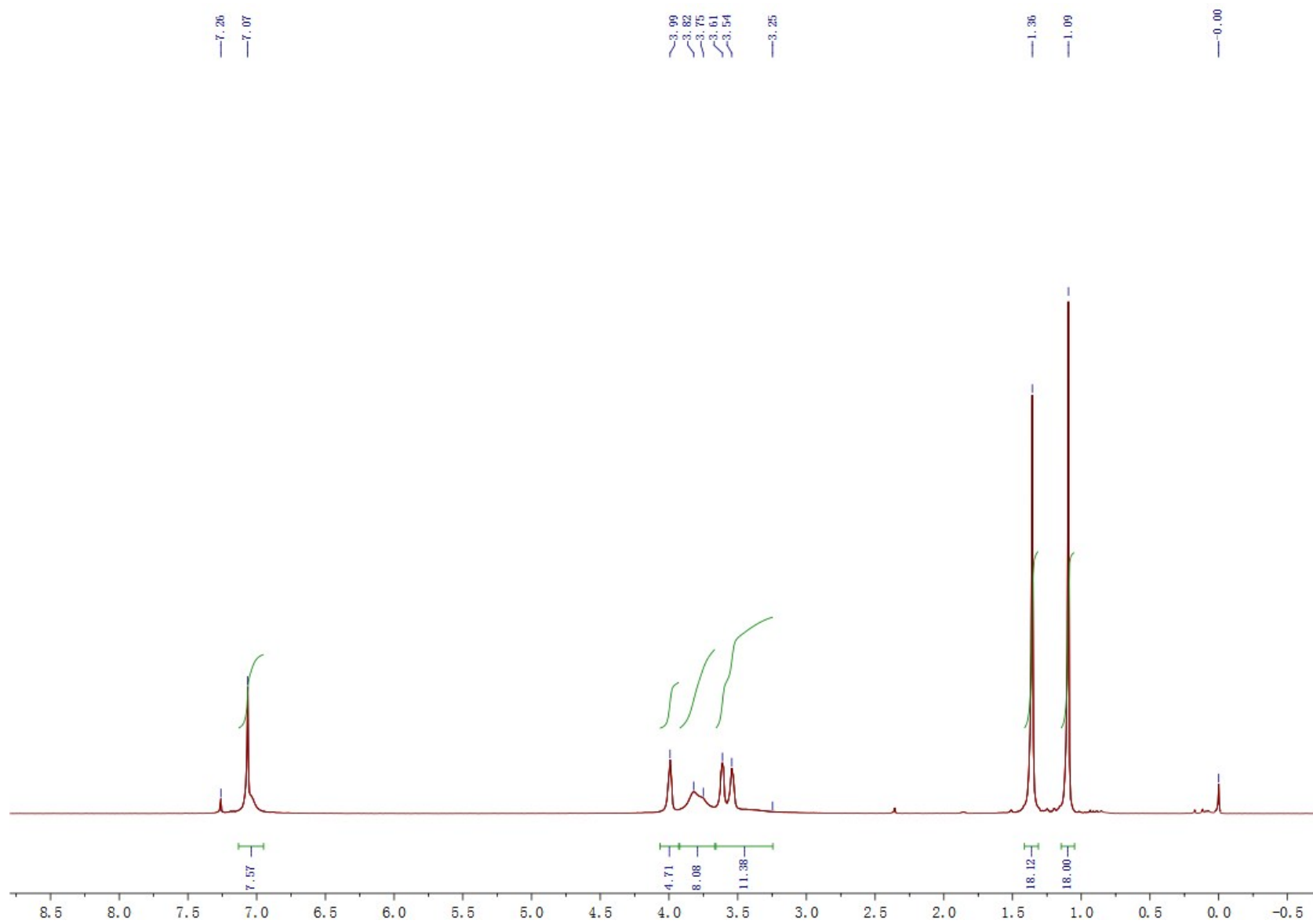


Figure S16. ^1H NMR spectrum (CDCl_3 , 25°C) of complex **3**.

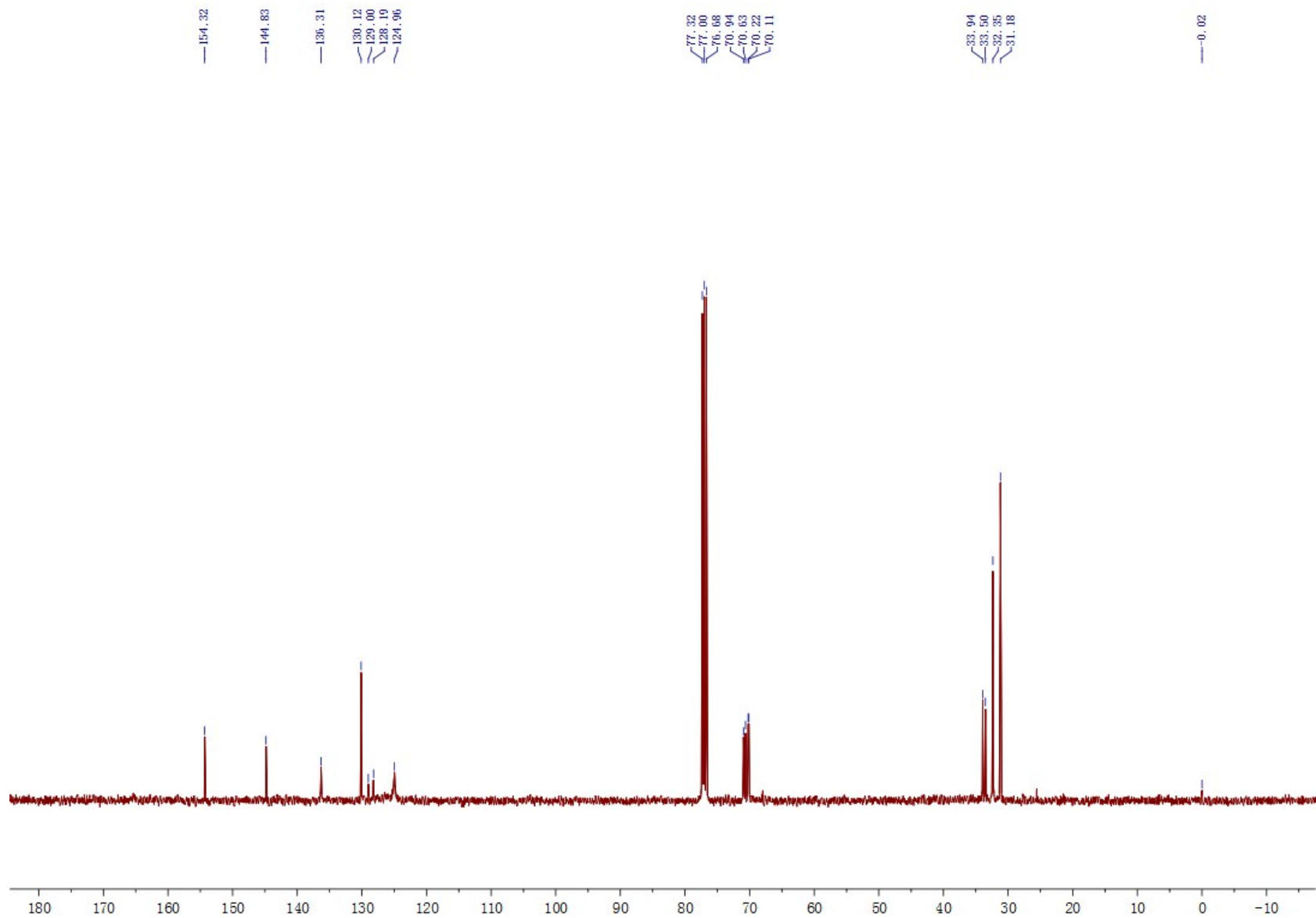


Figure S17. ^{13}C NMR spectrum (CDCl_3 , 25°C) of complex 3.

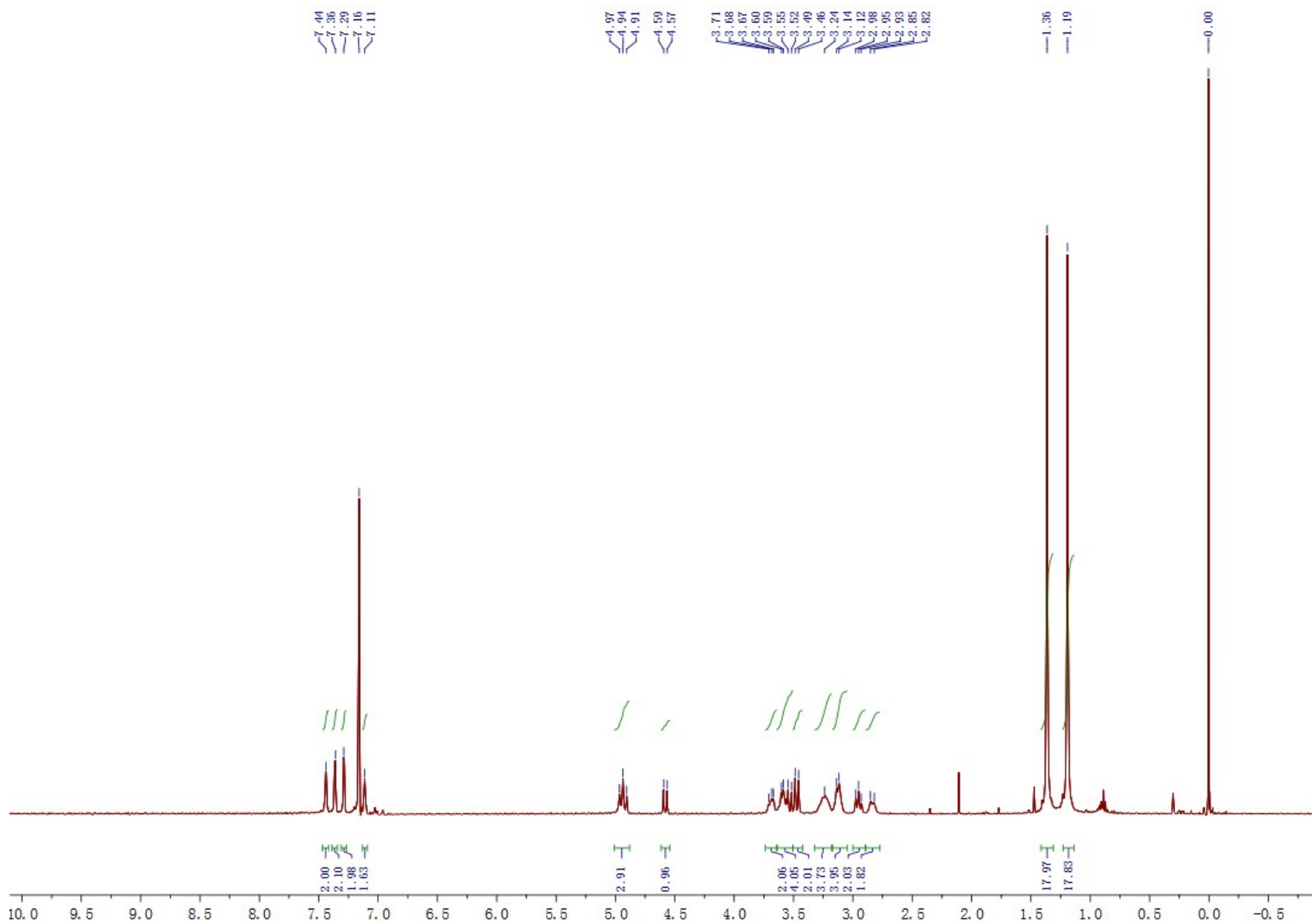


Figure S18. ^1H NMR spectrum (C_6D_6 , 25°C) of complex **4**.

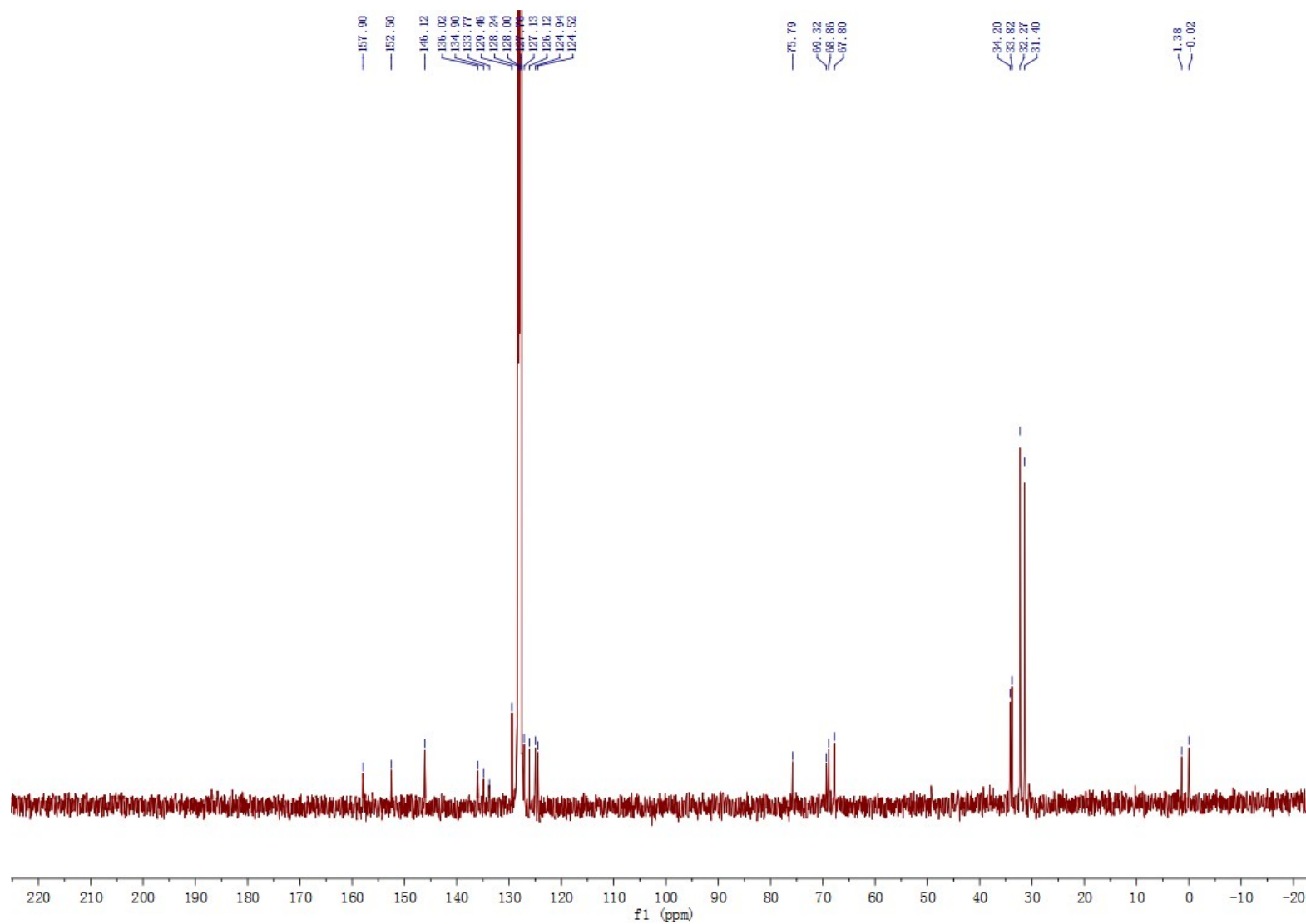


Figure S19. ^{13}C NMR spectrum (C_6D_6 , 25°C) of complex 4.

Table S1. Details of the X-ray structure Determinations of Complexes **1-4**.

	1	2	3	4
Formula	C ₅₀ H ₆₆ K ₂ O ₄	C ₆₂ H ₉₀ K ₂ O ₁₀	C ₅₂ H ₆₈ K ₂ O ₇	C ₅₂ H ₆₉ KO ₇ THF
Fw	808.23	1072.68	882.42	916.53
Temp	220.60(10)	173.00(10)	296(2)	293(2)
Crystal system	orthorhombic	monoclinic	monoclinic	monoclinic
Space group	Pnma	C2/c	P2 ₁	P2 ₁ /c
a Å	12.2579(5)	11.1093(3)	13.4859(10)	16.3022(3)
b Å	17.9504(9)	26.4085(9)	20.6897(15)	29.2158(5)
c Å	21.1486(6)	20.4600(7)	20.2255(15)	15.5007(3)
α°	90.00	90.00	90.00	90.00
β°	90.00(3)	92.614(3)	109.1440(10)	94.8725(19)
γ°	90.00	90.00	90.00	90.00
V Å ³	4653.4(3)	5996.3(3)	5331.2(7)	7356.0(2)
Z	4	8	2	4
Density(calcd) g·cm ⁻³	1.155	1.189	1.214	1.154
Absorb.coeff. mm ⁻¹	0.245	0.213	0.231	1.102
F(000)	1744	2320	2092	2784
Index ranges	-8 ≤ h ≤ 16 -23 ≤ k ≤ 24 -25 ≤ l ≤ 27	-14 ≤ h ≤ 14 -32 ≤ k ≤ 35 -15 ≤ l ≤ 25	-18 ≤ h ≤ 18 -19 ≤ k ≤ 29 -26 ≤ l ≤ 26	-17 ≤ h ≤ 19 -31 ≤ k ≤ 35 -18 ≤ l ≤ 18
Data/restr./param	5681/28/321	6823/84/373	15886/133/1276	13341/7/907
GOF	1.06	1.00	0.91	1.025

$[I > 2\sigma(I)]$	$R_1=0.086$ $wR_2=0.253$	$R_1=0.0497$ $wR_2=0.1156$	$R_1=0.060,$ $wR_2=0.133$	$R_1=0.068$ $wR_2=0.214$
CCDC number	1456971	1456970	1456968	1456969

References

(1) (a) Chamberlain, B. M.; Cheng, M.; Moore, D. R.; Ovitt, T. M.; Lobkovsky, E. B.; Coates, G. W. *J. Am. Chem. Soc.* **2001**, *123*, 3229. (b) Kasperczyk, J.; Bero, M. *Polymer* **2000**, *41*, 391.